Quantum Electronics **50** (7) 629–635 (2020)

https://doi.org/10.1070/QEL17276

Diffractive optical elements for multiplexing structured laser beams

N.L. Kazanskiy, S.N. Khonina, S.V. Karpeev, A.P. Porfirev

Abstract. **We consider methods for obtaining a multitude of structured laser beams (multiplexing) from an illuminating beam (both structured and unstructured) with the help of diffractive optical elements (DOEs). An approach of 'intelligent multiplexing' is proposed to describe and develop the methods. A DOE is calculated that forms a set of five diffraction orders located in a line. An example of focusing a set of doughnut-shaped azimuthally polarised laser beams using a diffraction beam splitter is presented. Efficient multiplexing of first-order vortex beams in a two-dimensional region is implemented by a two-dimensional diffraction grating. An approach is proposed and realised in which the transmission functions of a two-dimensional diffraction beam splitter and the elements forming structured laser beams with specified parameters are combined into the transmission function of one element. Such DOEs can be used in optical communication systems for encoding and decoding data. The possibility of using binary curved fork-shaped gratings for the formation of doughnut-shaped three-dimensional vortex beams, which are detected outside the focal plane, is demonstrated. This approach provides additional advantages for safe data transmission; it can be used in laser processing of materials and in laser manipulation applications.**

Keywords: *diffractive optical elements, structured laser beams, multiplexing, transmission function, diffraction orders.*

1. Introduction

Optical multiplexing of laser beams implies the formation of a multitude of both identical and different beams arranged in accordance with some pattern. Moreover, the structure of the pattern can be one-, two- or even three-dimensional. This significantly expands the capabilities of technologies used in such fields as laser manipulation [1], laser processing of materials [2] and optical communications [3]. Thus, the use of holographic optical tweezers in the form of several structured laser beams located at different points makes it possible to form a controlled fluid flow carrying arrays of nano- and microparticles along a given trajectory [4, 5], and the use of specified three-dimensional configurations of Gaussian beams allows one to produce various three-dimensional structures from captured microobjects [6–8]. When use is made of one- and two-dimensional arrays of various structured laser beams, it becomes possible to increase the processing speed of materials by several orders of magnitude in order to fabricate arrays of various nano- and microstructures, which are widely used in sensorics [9, 10]. The use of elements demultiplexing optical channels in communication lines can significantly increase the processing speed of incoming information in optical communications systems [11]. In optical communication systems, the demand for multiplexing and demultiplexing devices is determined by their ability to increase the throughput capacity of communication channels based on spatial division multiplexing (SDM), one of the varieties of which are mode division multiplexing (MDM) systems. An integral part of this idea is special optical elements for the analysis and formation of the transverse-mode composition of the light [12–16].

Currently, there are many approaches for calculating the elements generating single laser beams with desired properties, both iterative and non-iterative. To form sets of such beams, the calculated elements are usually combined with various diffractive optical elements (DOEs), for example, diffraction gratings [17–19] (Fig. 1). In this case, DOEs naturally produce multiple diffraction orders. Recently, many problems have arisen in which it is required to perform not only multiplexing of the initial beam into a multitude of such beams, but also to control their individual properties.

In this work, the general principles of the DOE design for the effective implementation of the intelligent multiplexing operation are systematically formulated. The methods for calculating the elements that multiplex the incident laser

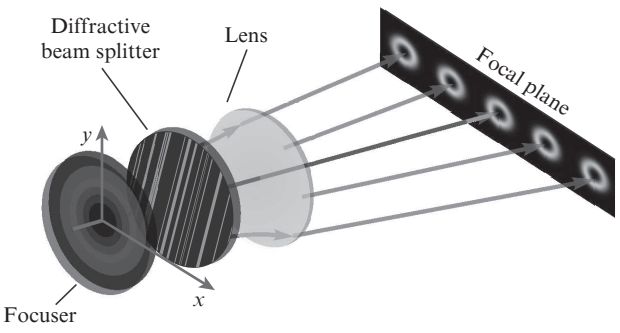

Figure 1. Formation of a one-dimensional array of doughnut-shaped light beams using a combination of a one-dimensional diffraction grating and a ring focuser.

N.L. Kazanskiy, S.N. Khonina, S.V. Karpeev, A.P. Porfirev Image Processing Systems Institute, Russian Academy of Sciences, Branch of the Federal Scientific Research Centre 'Crystallography and Photonics', Russian Academy of Sciences, ul. Molodogvardeiskaya 151, 443001 Samara, Russia; Samara University, Moskovskoe sh. 34, 443086 Samara, Russia; e-mail: porfirev.alexey@gmail.com

Received 11 February 2020; revision received 11 March 2020
Kvantovaya Elektronika **50** (7) 629–635 (2020)
Translated by I.A. Ulitkin

beam and form their specified one-, two- and three-dimensional configurations are analysed and compared. These methods can be easily adapted for calculating elements operating in various spectral (from sub-millimetre to nanometre) regions and can be used in practical applications.

2. Formation of one-dimensional configurations of laser beams

Laser beam multiplexing for producing a specified one-dimensional array of the beams is the simplest. In this case, it is necessary to control the distance between the beams being formed only in one coordinate. Consider an N-order diffraction beam splitter that can be easily used in combination with various structured laser beams. To calculate a DOE functioning as such a one-dimensional diffractive beam splitter, the superposition method with additional weighting coefficients can be used to control the energy directed to each diffraction order [20]. In this case, the element transmission function is calculated as

$$T(x,y) = \arg\left[\sum_{n=1}^{N} C_n \exp(\mathrm{i}v_{xn}x)\right], \quad (1)$$

where (x, y) are the Cartesian coordinates in the plane of the element; N is the number of generated orders; v_{xn} are the spatial frequencies of various diffraction orders that determine their actual position; arg [...] is the function of the argument; and C_n are complex coefficients that make it possible to redistribute energy between neighbouring diffraction orders. Spatial frequencies allow the position of all generated diffraction orders to be precisely controlled; in this case, any v_{xn} values can be used without any restrictions.

Consider an example of calculating a DOE, which forms a set of five diffraction orders located in a line. When the DOE is illuminated by any given structured laser beam, a set of five such beams will be generated, for example, in the form of doughnuts in the case of using an illuminating azimuthally polarised beam. The introduction of phase differences between adjacent diffraction orders by changing the coefficients C_n allows introducing destructive interference and weakening the higher diffraction orders. The centres of the corresponding diffraction orders in the Cartesian coordinate system are determined by the coordinates $x_n^{(c)} = \lambda f v_{xn}/2\pi$ and $y_n^{(c)} = 0$, where f is the focal length of the focusing system and λ is the wavelength of the used laser light. In calculating the C_n coefficients, we used the gradient method [21], which allowed us to calculate the diffractive beam splitter that generates light orders with high (about 0.98) uniformity.

To simulate the focusing of a set of doughnut-shaped azimuthally polarised laser beams based on the calculated diffractive beam splitter, we used the Richards–Wolf equation [22], which allows one to take into account the polarisation structure of the light field. The simulation took into account the fact that the laser beams are focused by a micro-lens with a numerical aperture NA = 0.5. Figure 2 shows the effect of a change in the period T_p between the centres of the neighbouring generated light rings on the root-mean-square error of their formation. The period T_p is in the range 0.6–3 μm, and the diameter of the light rings at a maximum intensity level is 0.9 μm. Figure 3 demonstrates good agreement between the experimentally and numerically obtained intensity distributions for all the considered periods T_p. The deviation in the distances between adjacent rings does not exceed 50 nm. In addition, the interference patterns obtained in these cases show that there are no significant changes in the phase structure of the generated fields.

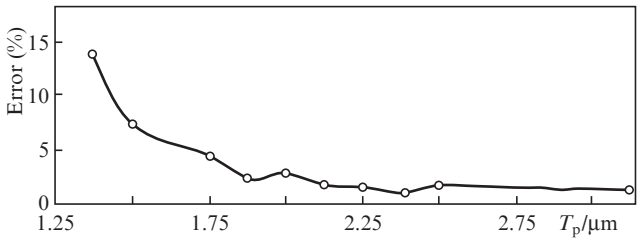

Figure 2. Root-mean-square error of the formation of light rings as a function of the period T_p.

To date, various methods for calculating one-dimensional diffractive beam splitters are known, including Dammann's method [23–26], iterative methods (for example, the Newton method [27–29] or the Gerchberg–Saxton algorithm [30, 31]), the gradient method, and various hybrid techniques [21]. The indicated methods make it possible to ensure high values of the efficiency and uniformity of the generated beams, due to which they are widely used in devices for laser processing of materials when high accuracy and uniformity of the generation of specified light fields are required. Thus, the use of one-dimensional binary light beam splitters made it possible to demonstrate printing of 10^7 functional structures per second

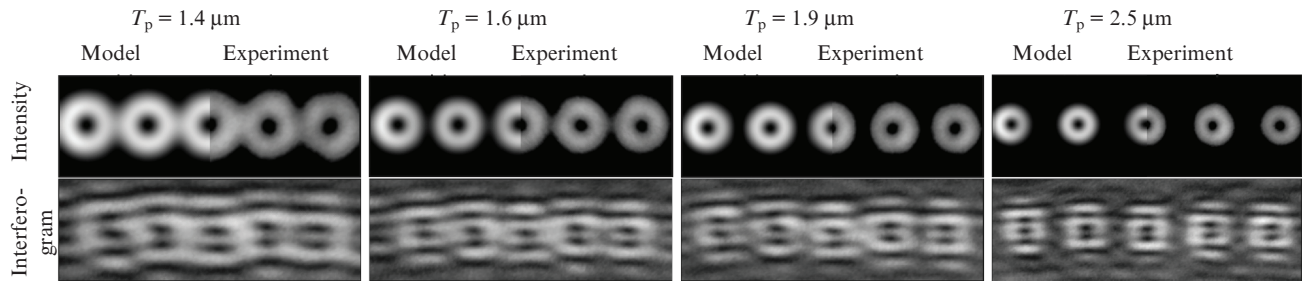

Figure 3. Numerically and experimentally obtained intensity distributions of doughnut-shaped laser beams formed by illumination of a diffractive beam splitter with an azimuthally polarised laser beam, as well as interferograms obtained for these fields as a result of their interference with a Gaussian beam with an oblique wavefront.

in thin films of gold [32], as well as to form arrays of microholes in stainless steel up to 30 μm thick [33].

3. Formation of two-dimensional configurations of laser beams

Modification of equation (1) by adding another spatial frequency v_{yn}, which sets the position of the generated diffraction order in the direction perpendicular to the given spatial frequency v_{xn}, allows it to be used to calculate two-dimensional beam splitters

$$T(x,y) = \arg\left[\sum_{n=1}^{N} C_n \exp(\mathrm{i}v_{xn}x + \mathrm{i}v_{yn}y)\right]. \quad (2)$$

It should be noted that in calculating such two-dimensional gratings, same iterative and enumeration methods are widely used as in the case of calculating one-dimensional gratings. First, the transmission function of a one-dimensional grating is calculated by iterative method, and then the transmission function of a two-dimensional grating is calculated as the product of the transmission functions of two one-dimensional gratings rotated by 90° relative to each other [18]. However, this approach allows one to calculate only diffractive beam splitters that form diffraction orders arranged in square and rectangular patterns. In this case, if we set $C_n = 1$ in equation (2), then in calculating the elements forming equidistant diffraction orders in Cartesian coordinates, there arises a situation for a large (more than 20) number of elements, when the intensity unevenness of the diffraction orders increases. A completely different situation takes place if the diffraction orders are arranged equidistantly in polar coordinates. It was shown in [34–36] that the ratio of the minimum intensity to the maximum one is approximately 0.62, compared with 0.34 in the case of Cartesian coordinates for 150 diffraction orders being generated.

As in the case of one-dimensional diffraction gratings, a two-dimensional grating successfully produces a set of diffraction orders if they are not too close to each other. When the diffraction orders separated by a distance comparable with their size are generated, the grating becomes very low-frequency and actually degenerates into an element to produce Hermite–Gaussian modes [37, 38] (Fig. 4). Such elements can be effectively used for multiplexing first-order vortex beams. In this case, the so-called Hermite–Gaussian beams with an embedded vortex are formed, which are described in the initial plane as [39]

$$\Psi_{nms} = \exp\left(-\frac{x^2+y^2}{2\sigma^2}\right) H_n\left(\frac{x}{\sigma}\right) H_m\left(\frac{y}{\sigma}\right)(x+\mathrm{i}y)^s, \quad (3)$$

where $H_n(x)$ and $H_m(y)$ are the Hermite polynomials of the nth and mth orders; σ is the size of the Gaussian beam waist; and s is the topological charge of the optical vortex embedded in the beam. The propagation of such a beam through a system of paraxial lenses can be described using the fractional Fourier transform [40] in polar coordinates:

$$E(\rho,\theta,z) = -\frac{\mathrm{i}k}{2\pi f \sin(\alpha z)} \exp(\mathrm{i}kz) \exp\left[\frac{\mathrm{i}k\rho^2}{2f\tan(\alpha z)}\right]$$
$$\times \int_0^{2\pi}\int_0^{R} E_0(r,\varphi) \exp\left[\frac{\mathrm{i}kr^2}{2f\tan(\alpha z)}\right]$$
$$\times \exp\left[-\frac{\mathrm{i}k\rho r}{f\sin(\alpha z)}\cos(\theta-\varphi)\right] r\,\mathrm{d}r\,\mathrm{d}\varphi, \quad (4)$$

where $\alpha = \pi/(2f)$, f is the focal length; $k = 2\pi/\lambda$ is the wave number; and R is the radius of the input beam. Figure 5 shows the propagation of Hermite–Gaussian beams with an embedded vortex from the initial plane ($z = 0$) through the focal plane of the optical system ($z = f = 300$ mm) to the output plane ($z = 2f = 600$ mm). It was previously theoretically shown that for $n = 1$ and $m = 1$, the light field formed in the focal plane is defined as [39]

$$F_{1,1,1}(\rho,\theta) = C_{1,1,1}\frac{2\pi^2}{\lambda f}\frac{k\rho\sigma^6}{f}\exp\left[-\frac{1}{2}\left(\frac{k\rho\sigma}{f}\right)^2\right]$$
$$\times \exp(\mathrm{i}\theta)\left[2\exp(-\mathrm{i}2\theta) + \mathrm{i}\left(\frac{k\rho\sigma}{f}\right)^2 \sin 2\theta\right]. \quad (5)$$

As follows from this equation, the intensity vanishes at the coordinate origin, as well as in the directions corresponding to 45, 135, 225, and 315°, i.e., at the vertices of the square (diagonally). An experimental study of such beams showed that the number of generated first-order vortex beams in this case is defined as $N = (n + 1)(m + 1) + nm$ (Fig. 6). Unfortunately, this approach cannot be applied to multiplexing vortex beams of a higher order. This is explained by the

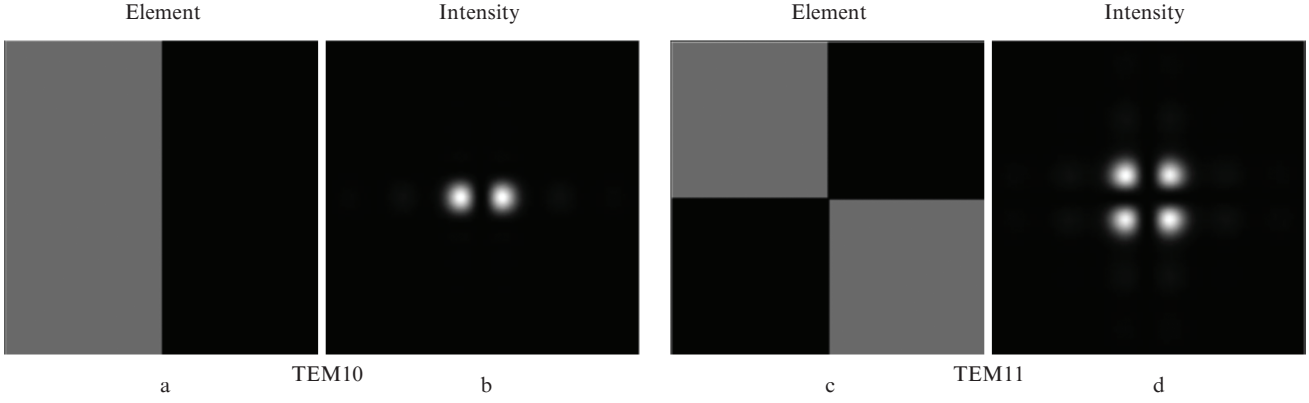

Figure 4. Examples of elements for the formation of Hermite–Gaussian modes TEM10 and TEM11: (a, c) their phase functions and (b, d) intensity distributions formed by them in the far zone.

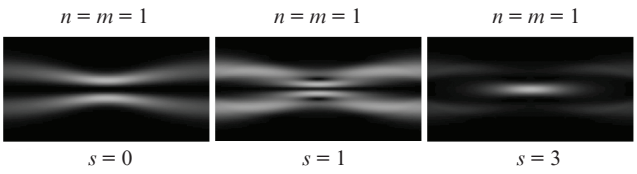

Figure 5. Transformation of Hermite–Gaussian beams with an embedded vortex passing through a lens system. The collecting lens is in the $z = 0$ plane.

fact that the diameter of the generated light rings increases with increasing vortex beam order. As mentioned above, the element for the formation of Hermite–Gaussian modes is actually a degenerate binary diffraction grating, which generates diffraction orders that are separated from each other by a distance comparable to their size. An increase in the diameter of multiplexed vortex beams and the presence of a phase delay between the generated diffraction orders leads in this case to the superposition of the initial multiplexed vortex beams and to distortion of the structure of the initial vortex beam.

Structured laser beams have been recently multiplexed using an approach in which the transmission functions of a two-dimensional diffractive beam splitter and elements forming structured laser beams with given parameters are combined into the transmission function of one element, for example, into the transmission functions of two-dimensional gratings and vortex/linear axicons [17, 33] or vortex beam shapers [41–45] (including perfect optical vortices [46]). In the latter case, this allows not only the formation of sets of different vortex beams in the required diffraction orders [47], but also the use of such elements for mode decomposition and analysis of the composition of the illuminating beam [48], for example, in optical communication systems for decoding data (including data encoded in cylindrically polarised beams) [49–52].

The use of the superposition method defined by equation (2) leads to a decrease in the diffraction efficiency of the formation of light fields with an increase in the number of generated orders. This can be avoided by the use of composite diffractive beam splitters, the area of which is divided into separate areas (both angular and radial sectors) with their own transmission function that deflects the incident beam to the required diffraction order [53–58]. These methods are non-iterative and also make it possible to control the polarisation of each generated laser beam from the set by adding an additional phase jump [53]. However, often such methods require high resolution in the manufacture of diffractive beam splitters, which increases the cost of their production.

4. Formation of three-dimensional configurations of laser beams

The next modification of the superposition method is to introduce into equation (1) another factor $\exp(\mathrm{i}kr^2/2f)$ that actually adds a spherical wavefront to a specific laser beam going in the (n, m)th diffraction order, which allows shifting the generated beam along its propagation axis:

$$T(x,y) = \arg\left[\sum_{n=1}^{N} C_n \exp\left(\mathrm{i}v_{xn}x + \mathrm{i}v_{yn}y + \mathrm{i}kr^2/2f\right)\right], \qquad (6)$$

where $r^2 = x^2 + y^2$.

This makes it possible to form predetermined three-dimensional configurations of laser beams. This approach has been considered in many papers [18, 59–62]. Three-dimensional diffractive beam splitters calculated on the basis of the Talbot effect work in a similar way [63]. However, in all these cases, as in the case of two-dimensional diffractive beam splitters calculated in accordance with the superposition method, the diffraction efficiency of the formation of diffraction orders decreases with increasing their

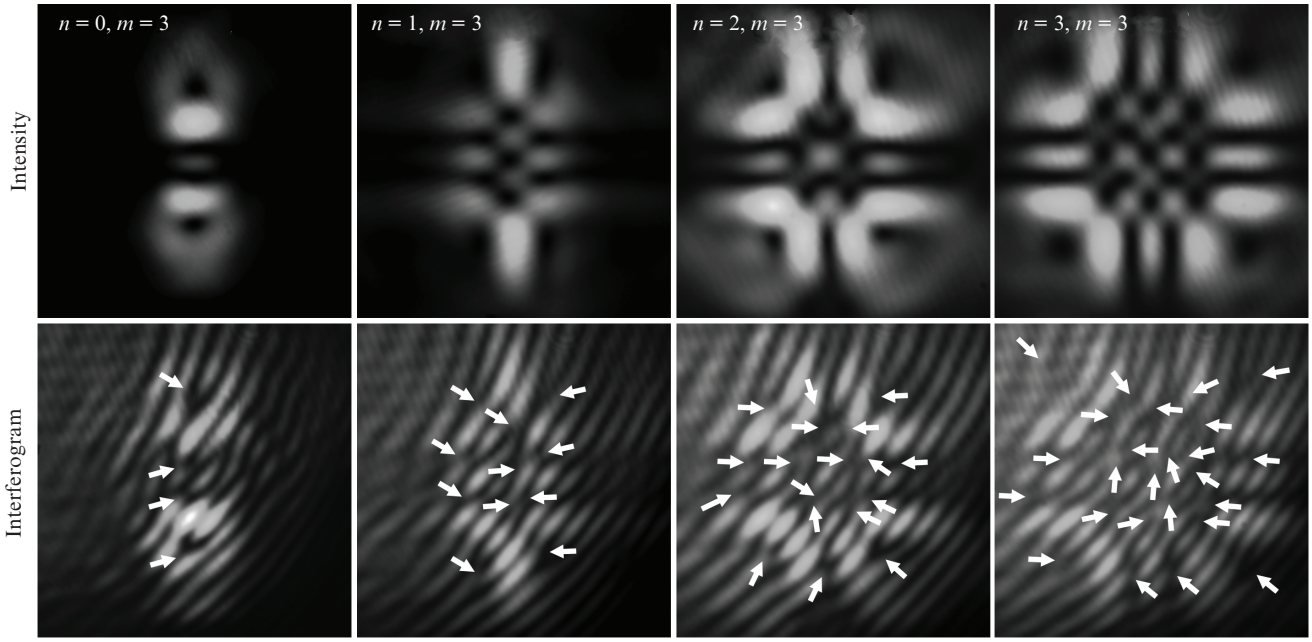

Figure 6. Experimentally obtained intensity distributions and interferograms of various Hermite–Gaussian beams with an embedded vortex. The arrows indicate the positions of the phase singularities in the interferogram patterns.

number, and, in addition, the phase structure of such elements has a rather irregular profile, which also complicates their manufacture.

There are simpler diffractive optical elements that can be used to form ordered three-dimensional arrays of structured laser beams, such as optical vortices. Such elements include the well-known spiral Fresnel zone plates and their various modifications (including so-called spiral Dammann zone plates [64]) and binary curved fork-shaped gratings.

A spiral Fresnel zone plate has the following transmission function:

$$T(x,y) = \exp\{\mathrm{i}\arg[\cos(\delta r^2 + p\varphi)]\}, \quad (7)$$

where (r, φ) are the polar coordinates in the plane of the element; $\delta = \pi/(\lambda f)$; f is the focal length of the first diffraction order formed by the spiral Fresnel zone plate illuminated by the light with a wavelength λ; and p is the topological charge of the vortex beam formed by the plate. The spiral Fresnel zone plate generates diffraction orders at various points along the propagation axis, and a vortex beam is formed in each of these orders, the topological charge of which is defined as pn, where n is the number of the diffraction order [65]. Moreover, such a plate can be used not only for the formation of various vortex beams, but also for their detection, since in this case the initial vortex beam with a topological charge l, illuminating the plate, is converted into a beam with a topological charge equal to $l + pn$ in the nth diffraction order (Fig. 7). The combination of a spiral Fresnel zone plate with a fork-shaped diffractive grating also allows the formation of optical vortex beams with different topological charges in different diffraction orders, located both along and across the propagation axis, thereby ensuring the generation of the specified beams in accordance with the required three-dimensional profile.

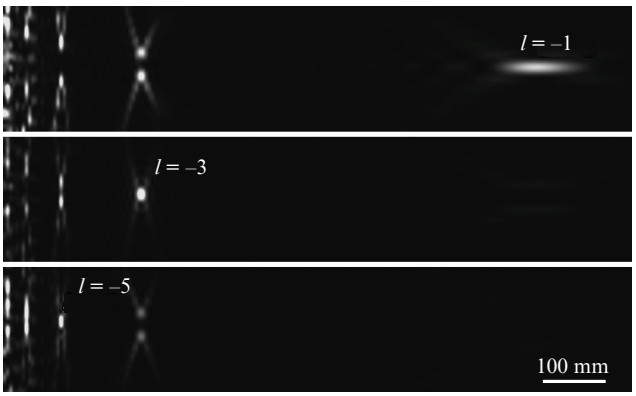

Figure 7. Simulated longitudinal sections of the intensity distributions of vortex beams with topological charges of –1, –3, and –5, passing through a spiral Fresnel zone plate with a topological charge $p = 1$.

Use of curved binary fork-shaped gratings with the transmission function of the form

$$\tau(r,\varphi) = \exp\left\{\mathrm{i}\frac{\pi}{2}(\mathrm{sgn}[\cos(\gamma r + \beta r\cos\varphi + m\varphi)] - 1)\right\}, \; r < R, \quad (8)$$

where γ is the quantity reciprocal to the axicon period, which is an integral part of this curved grating, and β is the spatial frequency of the carrier grating, also allows the formation of vortex beams in various three-dimensional configurations (m is the vortex order). Since the optical element defined by equation (8) is binary, not only ±1 diffraction orders are formed, but also other orders [66, 67], albeit with lower intensity. We write in explicit form the expansion of the transmission function of such a grating in a Fourier series:

$$\tau(r,\varphi) = \sum_{n=0}^{\infty} c_n \cos(n\gamma r + n\beta r\cos\varphi + nm\varphi)$$

$$= \sum_{n=-\infty}^{\infty} b_n \exp(\mathrm{i}n\gamma r + \mathrm{i}n\beta r\cos\varphi + \mathrm{i}nm\varphi), \quad (9)$$

where $c_n = 0$ for even orders n.

As follows from expression (9), each diffraction order corresponds to the formation of an optical vortex with the number nm. Moreover, the higher the diffraction order number n, the more it deviates from the optical axis: $n\beta r\cos\varphi = n\beta x$. Thus, diffraction orders 'scatter' in various directions. The presence of a conical wavefront $\exp(\mathrm{i}\gamma r)$ in the transmission function of this element and its transformation in each diffraction order into $\exp(\mathrm{i}n\gamma r)$ lead to the formation of doughnut-shaped distributions in the focal plane that are independent of the number of the optical vortex. The results of modelling the action of such a binary curved fork-shaped grating with a radius of 3 mm, supplemented by a lens with a focal length $f = 800$ mm and illuminated by a flat laser beam at a wavelength of 532 nm, are shown in Figs 8 and 9.

It can be seen from Figs 8 and 9 that the parameter γ is very important for shifting the maximum of the correspond-

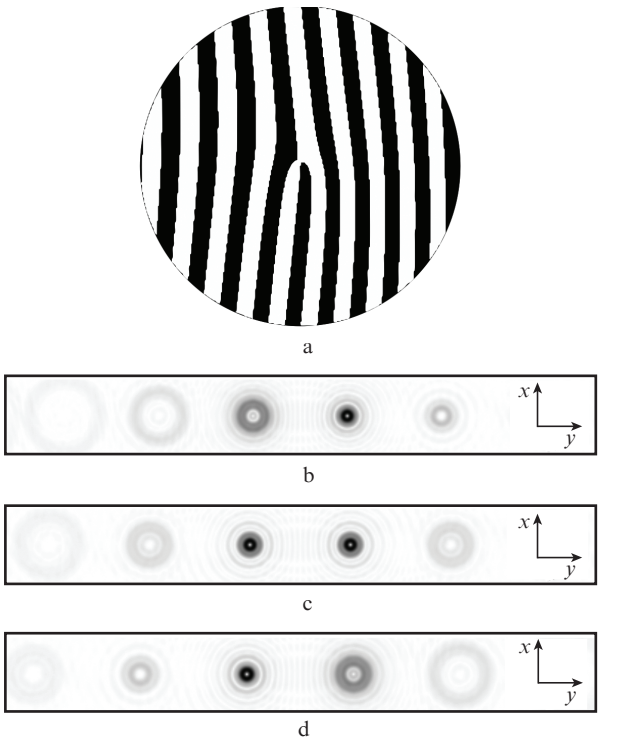

Figure 8. Formation of a set of vortex conical beams using a binary curved fork-shaped grating with $m = 1$, $\beta = 10$ mm^{-1} and $\gamma = 1$ mm^{-1}: (a) phase structure of the optical element and (b–d) patterns (negative images) of the transverse amplitude distribution ($x \in [-0.5$ mm, 0.5 mm], $y \in [-4$ mm, 4 mm]) at distances from the initial plane $z =$ (b) 772, (c) 800 (focal plane of the lens) and (d) 832 mm.

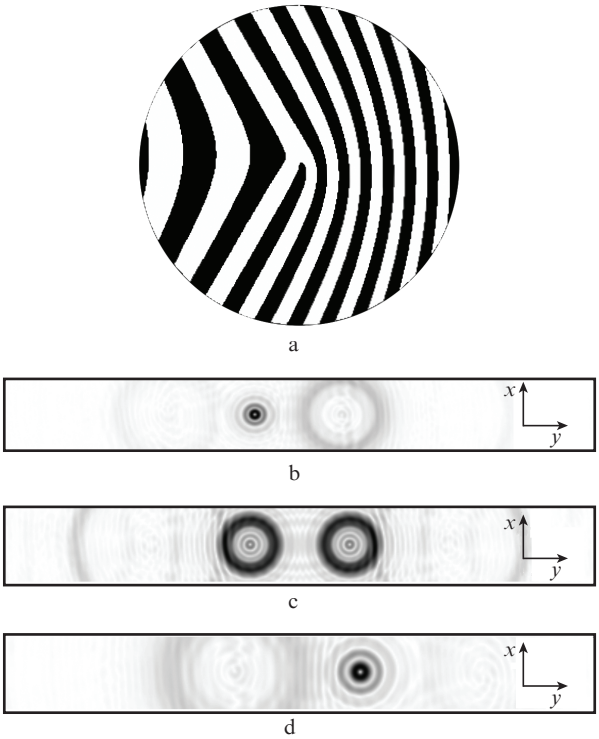

Figure 9. Same for a grating with $m = 1$, $\beta = 10$ mm^{-1} and $\gamma = 5$ mm^{-1}: (a) phase structure of the optical element, and (b–d) transverse amplitude distributions at $z =$ (b) 678, (c) 800 (focal plane of the lens) and (d) 915 mm.

ing diffraction order from the focal plane. The larger the value of γ, the greater the difference between the orders along the optical axis. Note also that the positive and negative diffraction orders are shifted in opposite directions, and the negative ones are shifted by a smaller distance than the positive orders of the same number. (This effect was observed earlier in [68].) In addition, at small values of the parameter γ, the formation of high diffraction orders is more pronounced, which is due to the coefficients of the Fourier series in expression (9). Obviously, in all cases, the maximum energy falls on the ±1st diffraction orders. However, using Dummann gratings or changing the level of binarisation of the grating [69], one can obtain gratings with a different fill factor and increase the energy contribution to other diffraction orders.

These results demonstrate the possibility of using binary curved fork-shaped gratings for the formation of three-dimensional configurations of vortex beams, the focusing of which occurs in different planes. The use of such a grating as a detector allows one to add another degree of freedom – a change in the coordinates of the correlation peaks along the optical axis. This approach provides additional benefits for secure data transmission. Note that the formation of three-dimensional configurations of doughnut-shaped vortex beams can also be used in laser processing of materials and in laser manipulation applications, for example, in single-pulse laser processing of bulk transparent materials to manufacture three-dimensional metamaterials [70] and to expand the functionality of holographic optical tweezers [71].

5. Conclusions

The methods for DOE synthesis to produce one-, two- and three-dimensional beam configurations are analysed. The possibilities of DOEs for forming quasi-periodic distributions consisting of many separate structured beams in given domains of space are demonstrated. Due to the use of the iterative superposition method with additional weighting factors for calculating the DOE functioning as a one-dimensional diffractive beam splitter, we have managed to obtain numerically and experimentally the intensity distributions of doughnut-shaped laser beams formed when the diffractive beam splitter is illuminated by a azimuthally polarised laser beam. The experimental results are in good agreement with the simulation results. Deviations in the distances between adjacent rings do not exceed 50 nm.

Methods for calculating two-dimensional diffraction gratings for the efficient multiplexing of first-order vortex beams are proposed. Such gratings enable to generate experimentally the so-called Hermite–Gaussian beams with an embedded vortex formed. The number of generated first-order vortex beams in this case is defined as $N = (n + 1)(m + 1) + nm$, where n and m are the orders of Hermite polynomials.

It is also shown that the addition of a spherical wavefront to a specific laser beam makes it possible to form specified three-dimensional configurations of laser beams. To implement this approach to the formation of ordered three-dimensional arrays of optical vortices, it is proposed to use spiral Fresnel zone plates and their various modifications. To form optical vortex beams with different topological charges in different diffraction orders, use is made of a combination of a spiral Fresnel zone plate with a fork-shaped diffraction grating. When this element was illuminated with a Gaussian beam, optical vortex beams with different topological charges in different diffraction orders are obtained, located both along and across the propagation axis. Such a plate can be used not only for the formation of various vortex beams, but also for the safe decoding of data in optical communication systems.

Additional prospects for the application of the methods in question provide the use of dynamic spatial light modulators for temporal modulation, which actually corresponds to the transition to 4D dimension.

Acknowledgements. This work was supported by the Russian Foundation for Basic Research (Project Nos 18-29-20045, 18-58-14001 and 18-07-00514) and by the Ministry of Science and Higher Education of the Russian Federation as part of the work on the State assignment of the Federal Research Center 'Crystallography and Photonics' of the Russian Academy of Sciences (Agreement No. 007-GZ/Ch3363/26). An experimental study of the formation of one-dimensional configurations of laser beams was carried out by A.P. Porfirev with the support of the Russian Science Foundation (Project No. 19-72-00018).

References

1. Grier D.G. *Nature*, **424** (6950), 810 (2003).
2. Kaakkunen J.J.J., Vanttaja I., Laakso P.J. *Laser Micro/Nanoeng.*, **9**, 37 (2014).
3. Abderrahmen T. et al. *IEEE Commun. Surv. & Tutor.*, **21**, 3175 (2019).
4. Ladavac K., Grier D.G. *Opt. Express*, **12**, 1144 (2004).
5. Būtaitė U.G. et al. *Nat. Commun.*, **10**, 1215 (2019).
6. Jordan P. et al. *Lab on a Chip*, **5**, 1224 (2005).
7. Kim K., Park Y.K. *Nat. Commun.*, **8**, 15340 (2017).
8. Tanaka Y. *Opt. Lasers Eng.*, **111**, 65 (2018).
9. Kudryashov S.I. et al. *Appl. Surf. Sci.*, **484**, 948 (2019).

10. Kudryashov S.I. et al. *Opt. Lett.*, **44**, 1129 (2019).
11. Lei T. et al. *Light: Sci. Appl.*, **4**, e257 (2015).
12. Golub M.A. et al. *Sov. J. Quantum Electron.*, **12**, 1208 (1982) [*Kvantovaya Elektron.*, **9**, 1866 (1982)].
13. Golub M.A. et al. *Sov. J. Quantum Electron.*, **13**, 1123 (1983) [*Kvantovaya Elektron.*, **10**, 1700 (1983)].
14. Golub M.A. et al. *Sov. J. Quantum Electron.*, **14**, 1255 (1984) [*Kvantovaya Elektron.*, **11**, 1869 (1984)].
15. Golub M.A. et al. *Sov. J. Quantum Electron.*, **18**, 392 (1988) [*Kvantovaya Elektron.*, **15**, 617 (1988)].
16. Dubois F. et al. *Opt. Lett.*, **19**, 433 (1994).
17. García-Martínez P. et al. *Appl. Opt.*, **51**, 1375 (2012).
18. Zhu L. et al. *Opt. Express*, **22**, 21354 (2014).
19. Fu S. et al. *J. Opt. Soc. Am. A*, **33**, 1836 (2016).
20. Di Leonardo R. et al. *Opt. Express*, **15**, 1913 (2007).
21. Glotov P.A., Kotlyar V.V. *Computer Optics*, **19**, 74 (1999) [*Komp'yuternaya Opt.*, **19**, 74 (1999)].
22. Richards B., Wolf E. *Proc. R. Soc. Lond. A*, **253**, 358 (1959).
23. Dammann H., Gortler K. *Opt. Commun.*, **3**, 312 (1971).
24. Dammann H., Klotz E. *Opt. Acta*, **24**, 505 (1977).
25. Jahns J. et al. *Opt. Eng.*, **28**, 1267 (1989).
26. Turunen J. et al. *Opt. Eng.*, **28**, 1162 (1989).
27. Feldman M.R., Guest C.C. *Opt. Lett.*, **14**, 479 (1989).
28. Krackhardt U., Streibl N. *Opt. Commun.*, **74**, 31 (1989).
29. Mait J.N. *J. Opt. Soc. Am. A*, **7**, 1514 (1990).
30. Bereznyi A.E., Komarov S.V., Prokhorov A.M., Sisakyan I.N., Soifer V.A. *Dokl. Akad. Nauk SSSR*, **287** (3), 623 (1986).
31. Doskolovich L.L., Bezus E.A., Bykov D.A., Skidanov R.V., Kazanskiy N.L. *Computer Optics*, **43** (6), 946 (2019) [*Komp'yuternaya Opt.*, **43** (6), 946 (2019)]; DOI: 10.18287/2412-6179-2019-43-6-946-955.
32. Pavlov D. et al. *Opt. Lett.*, **44**, 283 (2019).
33. Kuang Z. et al. *J. Phys. D: Appl. Phys.*, **47**, 115501 (2014).
34. Doskolovich L.L., Bezus E.A., Kazanskiy N.L. *Computer Optics*, **42** (2), 219 (2018) [*Komp'yuternaya Opt.*, **42** (2), 219 (2018)]; DOI: 10.18287/2412-6179-2018-42-2-219-226.
35. Kazanskiy N.L., Skidanov R.V. *Appl. Opt.*, **51**, 2672 (2012).
36. Hermerschmidt A. et al. *Opt. Lett.*, **32**, 448 (2007).
37. Khonina S.N. *Computer Optics*, **18**, 28 (1998) [*Komp'yuternaya Opt.*, **18**, 28 (1998)].
38. Karpeev S.V., Podlipnov V.V., Ivliev N.A., Paranin V.D. *Computer Optics*, **43** (3), 368 (2019) [*Komp'yuternaya Opt.*, **43** (3), 368 (2019)]; DOI: 10.18287/24126179-2019-43-3-368-375.
39. Porfirev A.P., Khonina S.N. *Opt. Express*, **25**, 18722 (2017).
40. Alieva T. et al. *EURASIP J. Adv. Signal Process.*, **10**, 1 (2005).
41. Wang Z. et al. *Opt. Express*, **19**, 482 (2011).
42. Fu S. et al. *Appl. Opt.*, **55**, 1514 (2016).
43. Zhang N. et al. *Opt. Lett.*, **35**, 3495 (2010).
44. Fu S. et al. *Opt. Express*, **24**, 6240 (2016).
45. Davis J.A. et al. *Appl. Opt.*, **53**, 2040 (2014).
46. Deng D. et al. *Opt. Express*, **24**, 28270 (2016).
47. Porfirev A.P. et al. *Sci. Rep.*, **6**, 1 (2016).
48. Fu S. et al. *Appl. Opt.*, **57**, 1056 (2018).
49. Fu S. et al. *Opt. Express*, **27**, 33111 (2019).
50. Fu S. et al. *OSA Continuum*, **1**, 295 (2018).
51. Li S., Wang J. *Opt. Express*, **25**, 21537 (2017).
52. Khonina S.N. et al. *Opt. Express*, **27**, 18484 (2019).
53. Zhu L. et al. *Opt. Express*, **23**, 24688 (2015).
54. Deng D. et al. *Opt. Commun.*, **382**, 559 (2017).
55. Li P. et al. *Sci. Rep.*, **8**, 9831 (2018).
56. Mu T. et al. *Opt. Lett.*, **41**, 261 (2016).
57. Ren H. et al. *Opt. Lett.*, **39**, 6771 (2014).
58. Guan J. et al. *Opt. Express*, **26**, 24075 (2018).
59. Yu J. et al. *Appl. Opt.*, **51**, 2485 (2012).
60. Yu J. et al. *Appl. Opt.*, **51**, 1619 (2012).
61. Zhu L. et al. *Opt. Express*, **25**, 24756 (2017).
62. Davis J.A. et al. *Appl. Opt.*, **50**, 3653 (2011).
63. Zhu L. et al. *Opt. Express*, **22**, 9798 (2014).
64. Yu J. et al. *Appl. Opt.*, **51**, 6799 (2012).
65. Soskin M.S. et al. *New J. Phys.*, **6**, 196 (2004).
66. Mait N. *J. Opt. Soc. Am. A*, **7**, 1514 (1990).
67. Borghi R. et al. *J. Opt. Soc. Am. A*, **17**, 63 (2000).
68. Khonina S.N. et al. *J. Opt. Soc. Am. A*, **36**, 1039 (2019).
69. Khonina S.N., Ustinov A.V. *Appl. Opt.*, **58**, 8227 (2019).
70. Ni J. et al. *Light Sci. Appl.*, **6**, e17011 (2017).
71. Garcés-Chávez V. et al. *Nature*, **419**, 145 (2002).